Saidi et al. 2018. *Int. J. Vehicle Structures & Systems*, 10(4), 263-267
ISSN: 0975-3060 (Print), 0975-3540 (Online)
doi: 10.4273/ijvss.10.4.07

International Journal of Vehicle Structures & Systems
Available online at www.maftree.org/eja

Study and Realization of a Driver Assistive System for Control of Instantaneous Center of Rotation in an Electric Vehicle

Hemza Saidi[a] and Djebri Boualem[b]

[a]*Dept. of Electrical Engg., Mohamed Boudiaf University of Sci. and Tech., Oran, Algeria*
Corresponding Author, Email: hamzaing2008@yahoo.fr
[b]*Laboratory for City, Architecture and Heritage, Polytechnique School of Architecture and Town planning, Algeria*
Email: h.saidi@univ-chlef.dz

ABSTRACT:

The stability of electric vehicles is difficult during their mobility on a curved trajectory with several driving wheels. This problem causes a danger for the electric vehicle stability due to the effect of the instantaneous center of rotation (ICR). The desire to have more safety in this type of vehicle encourages us to develop a driving assistive system to reduce the effects of ICR in two wheels drive electric vehicles using Arduino and a LabVIEW interface for data processing that help to control the vehicle on the road. Analytical solutions and their implementations are demonstrated through experimental testing in a laboratory scale.

KEYWORDS:

Driver assistive technologies; Electric vehicle; Instantaneous center of rotation; Stability and control

CITATION:

H. Saidi and D. Boualem. 2018. Study and Realization of a Driver Assistive System for Control of Instantaneous Center of Rotation in an Electric Vehicle, *Int. J. Vehicle Structures & Systems*, 10(4), 263-267. doi:10.4273/ijvss.10.4.07.

ACRONYMS AND NOMENCLATURE:

Bg, Bd	Steering angle of the front left & right wheel
Bb	Steering angle in bicycle mode
L	Length of vehicle wheelbase
R	Radius of the back train ICR
Rf	Radius of ICR +Back train displacement
H	Vehicle length
Rcg	Radius of curvature of the mass center
$L1$, $L2$	Front & back half-wheelbase
Bcg	Steering angle of the mass center
Δ	Trajectory's split of the back train
Af, Ar	Drift angle of the front & back train
Fyf, Fyr	Front & back train lateral force
m	Vehicle mass
V	Forward speed
Cαf, Cαr	Rigidity co-efficient of the lateral force of the front and back train

1. Introduction

The instantaneous axis of rotation is a term used in classical mechanics and more particularly in kinematics in order to designate the axis around which a solid is rotating at a given instant with respect to a reference frame. If we can use the simplification of plane problems, we talk about instantaneous center of rotation (ICR). When a solid isolated in the mechanical sense of the term moves according a trajectory in a plane, the ICR is defined as the point where the velocity vector is zero. The ICR lies on the perpendicular to each velocity vector of the isolated solid passing through the point of application of the latter. When the isolated solid moves only in translation in a plane, the ICR is projected to the infinity. The notion of a triangle of velocities allows to determine the velocity vector at any point of the solid, provided that we know the velocity vector at a point and the position of the ICR [1-2].

2. Movement in low speed steering

According to the Ackermann model illustrated in Fig. 1, when $\beta g \leq \beta d$ the steering angles of the front wheels are given by,

$$Tan\,\beta d = L/(h - h/2) \quad (1)$$

$$Tan\,\beta g = L/(R + h/2) \quad (2)$$

$$1cot\,\beta g - cot\,\beta d = h/L \quad (3)$$

On the other hand, for the bicycle model as illustrated in Fig. 2 gives, the steering angle of the front wheel is given by Tan $\beta b = L / R$. Then Eqn. (3) becomes,

$$Cot\,\beta b = (cot\,\beta g + cot\,\beta d)/2 = R/L \quad (4)$$

The center of radius of curvature is given by,

$$Rcg = \sqrt{L_2^2 + R^2} = \sqrt{L22 + L^2\,cot^2\,\beta b} \quad (5)$$

$$Rcg = R\sqrt{1 + L22/R^2} \approx (1 + L22R2) \approx R \quad (6)$$

Relationship between the curvature and the steering angle with $Rcg \approx R \approx L \cot \beta b \approx L\beta b$ is given by,

$$cot\,\beta b = R/L \quad (7)$$

Then we will have B$b = L / R$. The arc length of the mass center is given by,

$$\beta cg = arc\,tan\left(\frac{L2}{R}\right)\beta cg = arc\,sin\left(\frac{L2}{R}\right) = arc\,sin\,(L2\sqrt{R2 + L_2^2}) = L2/L\beta b \quad (8)$$

$$\beta cg = L2 / L\beta b \quad (9)$$

The displacement of the rear wheel trajectory is given by,

$$Rf = \sqrt{R2 + L^2} \quad (10)$$

$$\Delta = Rf - R = (\sqrt{1 + L^2 / R^2} / -1) \quad (11)$$

We have that: $\sqrt{1 + x2} \approx 1 + x/2 + \ldots$ and $\Delta = L^2 / 2R$.

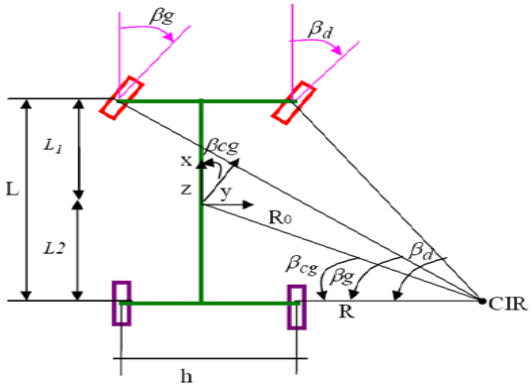

Fig. 1: Ackerman steering model

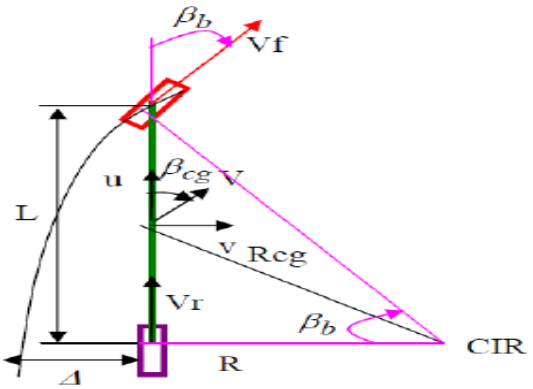

Fig. 2: Ackerman bicycle model

3. Movement in high speed steering

The study of movement of the vehicle in high speed steering involves a hypothesis to take into account the drift angle of the front and back wheels. Fig. 3 illustrates the movement of bicycle using high speed steering model. From Fig. 3, we can deduce the steering angle as a function of the drift angle using,

$$Bb = L/R + \alpha f - \alpha r \quad (12)$$

The equations of motion for the tire as per Fig. 4 are,

$$Fyf = C\alpha f \, \alpha f \qquad Fyr = C\alpha r \, \alpha r \quad (13)$$

The equations of lateral equilibrium and rotation are given by,

$$Fyf \cos \beta b + Fyr = mV2 / R \quad (14)$$

$$Fyf \cos \beta bb + FyrL2 = 0 \quad (15)$$

By using small angle hypothesis, the above equations can be simplified further as follows,

$$Fyf = (L2 / L)\, m\, (V2 / R) \quad (16)$$

$$Fyr = (L1 / L)\, m\, (V2 / R) \quad (17)$$

$$Fyf = f\alpha f \, \alpha f = (L2 / L)\, m\, (V2 / R) \quad (18)$$

$$Fyr = r\alpha r \, \alpha r = (L1 / L)\, m\, (V2 / R) \quad (19)$$

Through simplification and reordering, we obtain,

$$\alpha f / \alpha r = L2\, C\alpha r / L1\, C\alpha f \quad (20)$$

The steering angle according to speed and steering abruptness is obtained as follows,

$$Bb = L / R + ((mL2 / C\alpha f) - (mL1 / C\alpha r\, L))\, V2/R \quad (21)$$

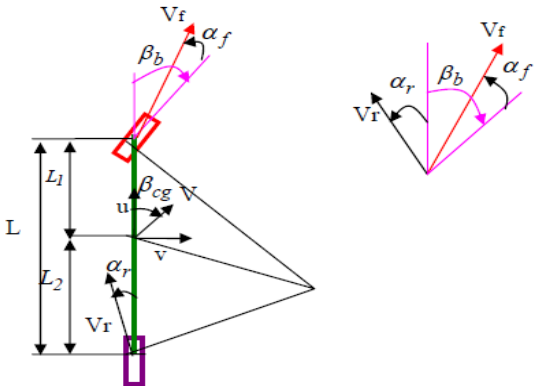

Fig. 3: Representation of the high-speed bicycle model

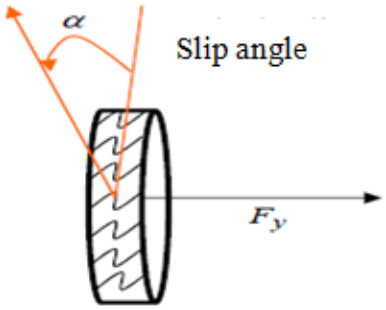

Fig. 4: Behaviour of the tire

4. System modelling & simulation

It is necessary to maintain the velocity at a determined value in the presence of the external or internal perturbations as their influence is inherently variable. Proportional-Integral (PI) controller is implemented using a microcontroller-based system. Fig. 5 illustrates the various components of the proposed system. The DC motor model SE-2662-5A from manufacturer NL (Lucas-Nuelle) is used. This motor has an external diameter of 40mm, a length of 86.2mm, a power of 1 kW and a nominal supply voltage of 220VDC. It can run at 2100 tr/min and requires an IErr current of 0.24A. For the armature, a nominal supply voltage of 220VDC and a nominal current of 6.2A are required. The motor is controlled by pulse width modulation (PWM) signals generated by the microcontroller.

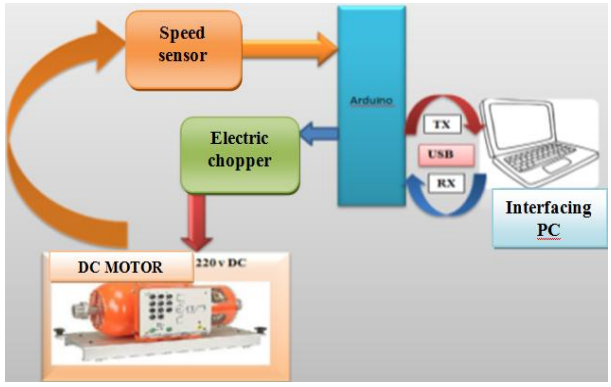

Fig. 5: Synoptic diagram of the test bench

To identify a real dynamic system, is to characterize another system based on the experimental knowledge of inputs and outputs in order to obtain an identical behaviour. To accomplish this, graphic and statistical methods [1-2] are available. Arduino card is used as an interface card between the system and the computer. The computer is equipped with a LabVIEW interface enabling it to acquire and store input and output samples as shown in Fig. 6 [3]. The (.lvm) file is designed such that it facilitates parsing the reading when imported into a spreadsheet. The identification operation tool to find the mathematical model is shown in Fig. 7. Fig. 8 shows an overview of the interface between LabVIEW and MATLAB tool [5]. When the system is excited with a step input U(k), the system response Y (k) is obtained as shown in Fig. 9. The sampling time Ts = 0.1 s. The continuous transfer function of the system for identification, as shown in Fig. 10, is given by,

$$G\,(s)\;=\;\frac{9.79}{1+0.29S} \tag{22}$$

The PI controller can be established using,

$$u(t) = K_P\left(\varepsilon(t) + K_i\int_0^t \varepsilon(t)dt\right) \tag{23}$$

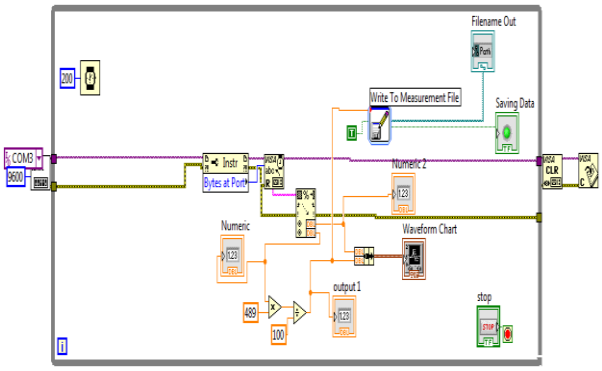

Fig. 6: Block diagram of a serial flow

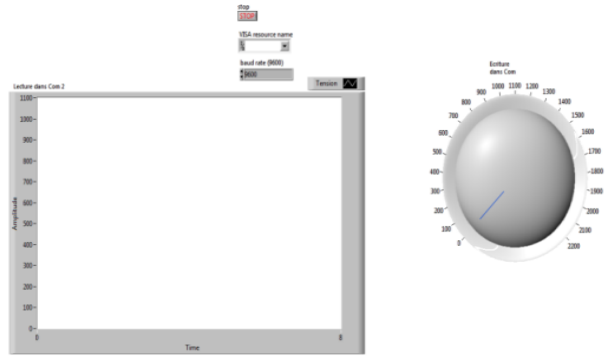

Fig. 7: Acquisition tool interface

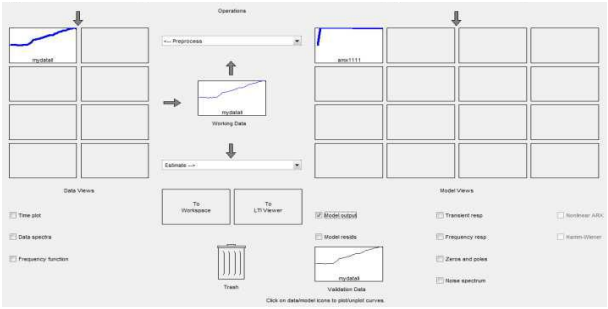

Fig. 8: Identification tool interface

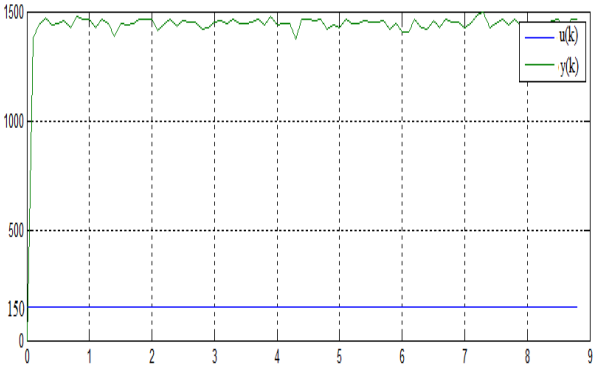

Fig. 9: Response of the system to a step input

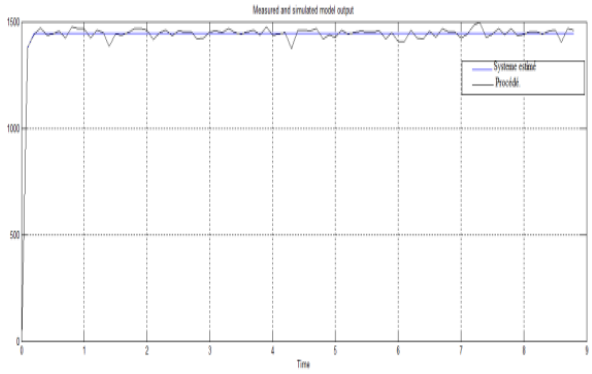

Fig. 10: System estimated response by its transfer function

The PI controller can be established using,

$$u(t) = K_P\left(\varepsilon(t) + K_i\int_0^t \varepsilon(t)dt\right) \tag{23}$$

The transfer function of the controller is then given by,

$$\mathrm{C(p)} = \frac{K_P S + K_i}{s} \tag{24}$$

The parameters of the regulator are defined as a function of the damping ζ and the pulsation ω_n using,

$$K_i = \frac{\omega_n 2\tau}{k} \tag{25}$$

$$K_p = \frac{2\xi\omega_n\tau - 1}{k} \tag{26}$$

$$\omega_n = \frac{5}{\xi t_r} \tag{27}$$

After calculating the parameters for the PI controller, the system simulation is carried out using Matlab/Simulink. The results of the simulation are presented in Fig. 11.

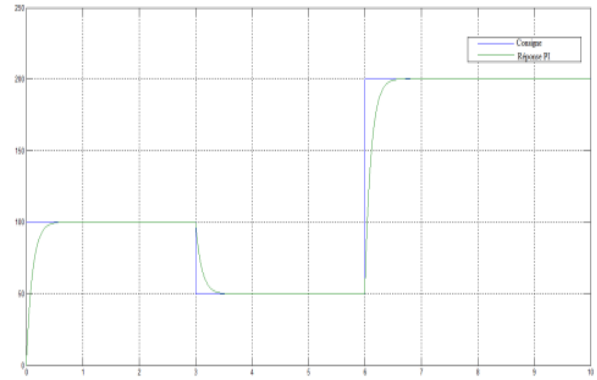

Fig. 11: Set point tracking (simulation) and rejection of perturbations with PI

Fig. 12 illustrates the behaviour of the system after the implementation of the digital PI controller. At first, we gave a set point of N = 1500tr/min, we note that the

output of the system follows this instruction. Then we came down to N = 500tr/min. We also notice that the output of the system follows. Finally, with set point of N = 1000 tr/min, the same desired behaviour was obtained. The PI regulator has given satisfactory results.

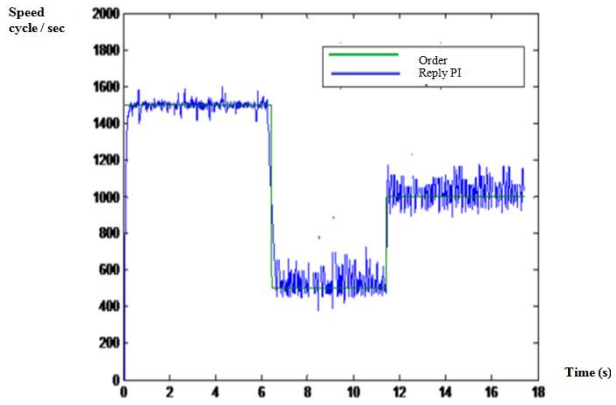

Fig. 12: Set point tracking (experiment) and process behaviour with a digital PI

5. Practical realization

The designed system is tested to decrease the effect of the ICR in an electric vehicle [4]. The synoptic diagram is composed of control part (PC interface), control circuit and electronic part as shown in Figs. 13-16. After the practical realization of the system as shown in Fig. 17, experiments are carried out for linear steering, steering right and steering right manoeuvres. When the steering wheel is at level 1, no rotation of the steering wheel is observed as shown in Fig. 18. When turning the steering wheel to the right, the responses for various ICR are shown in Figs. 19(a) to (c). When turning the steering wheel to the right, the duty cycle (between 1 - 2) of the PWM signal given to the right engine decreases its speed and the second motor remains constant.

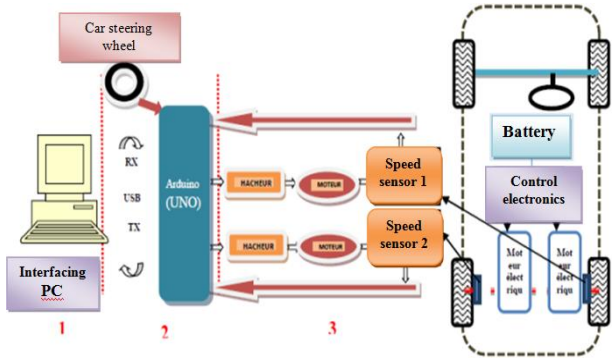

Fig. 13: Synoptic diagram of designed system

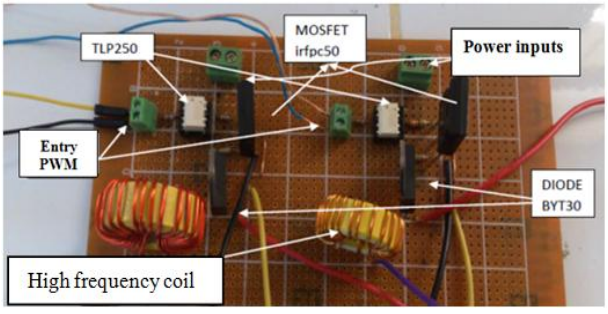

Fig. 14: Realization of the series circuit

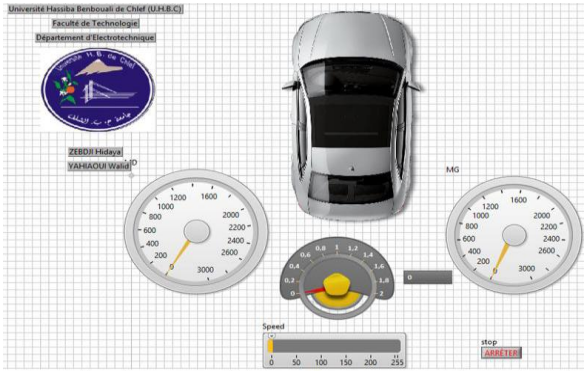

Fig. 15: Front panel of design assistive system interface

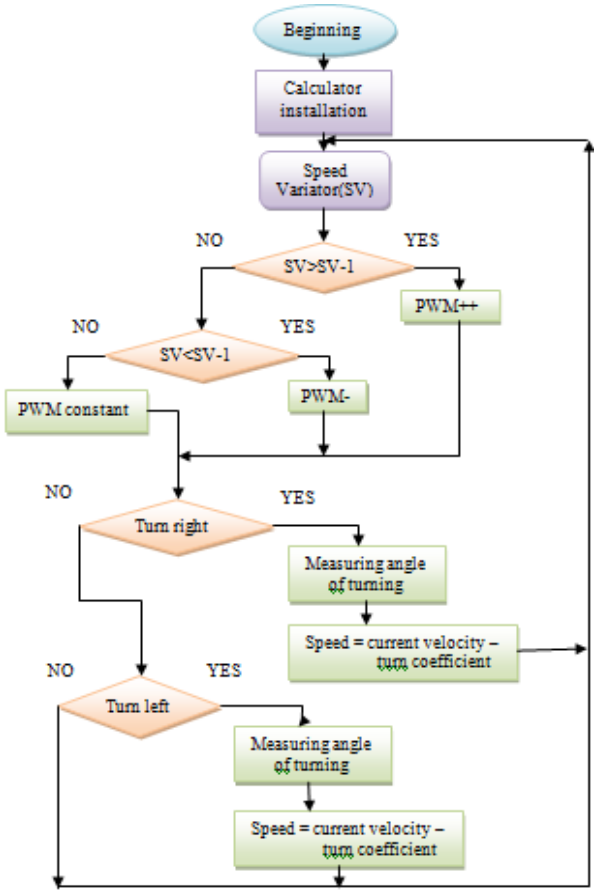

Fig. 16: Flow chart for the realised design assistive system

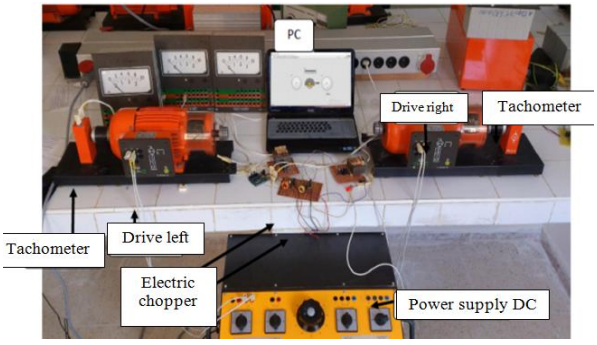

Fig. 17: Assembly of the designed system

When turning the steering wheel to the left, the responses for various ICR are shown in Figs. 20(a) to (c). When the steering wheel is turned to the left, the duty cycle (which lies between 1-0) of the PWM signal given to the left engine decreases its speed and the second motor remains constant.

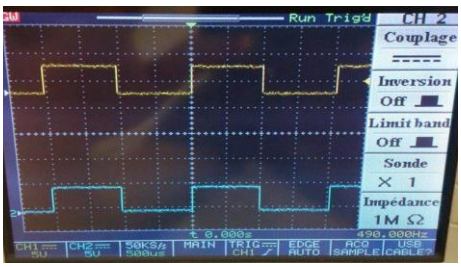

Fig. 18: Steering wheels in position 1

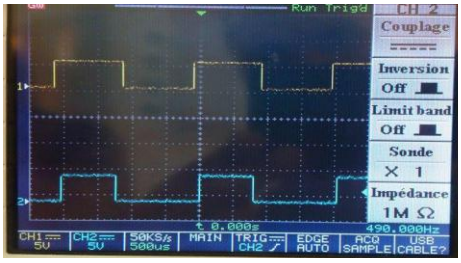

Fig. 19(a): Steering wheel in position [1.1-1.5]

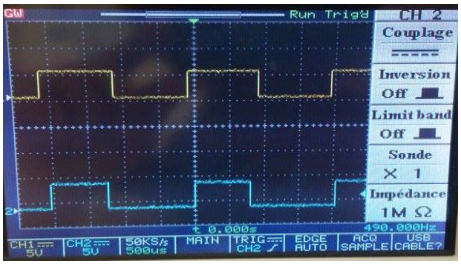

Fig. 19(b): Steering wheel in position [1.5-1.8]

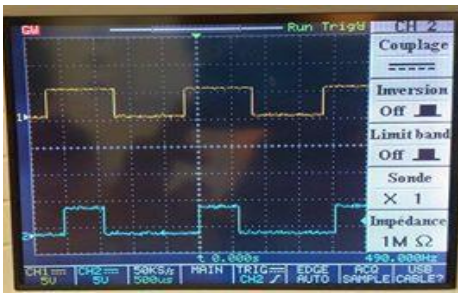

Fig. 19(c): Steering wheel in position greater than 1.8

Fig. 20(a): Steering wheel in position [0.9-0.5]

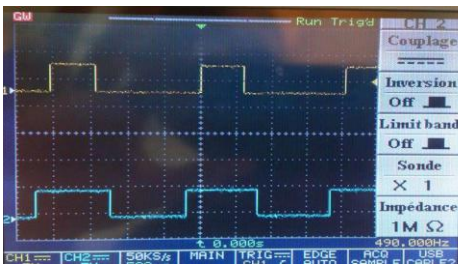

Fig. 20(b): Steering wheel in position [0.5-0.2]

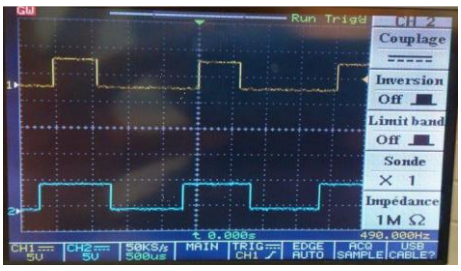

Fig. 20(c): Steering wheel in position below 0.2

6. Conclusion

The study and realization of a system that reduces the effects of the ICR in an electric vehicle was presented. We used a Lab view interface to transmit the signals to the motors (the wheels) and when turning the potentiometer (steering wheel) we noticed the variation of the speed of the vehicle with the conditions that we targeted. This has enabled the driver assistive system towards semi-autonomous or mobility vehicles with a user friendly interface.

REFERENCES:

[1] H. Saidi. 2010. *Etude et Réalisation d'un Véhicule Solaire*, Master Thesis (in French), University of Sci. and Tech. of Oran-Mohamed Boudiaf, Algeria.

[2] Z.B. Ibrahim, M.L. Hossain, I.B. Bugis, J.M. Lazi and N.M. Yaakop. 2014. Comparative analysis of PWM techniques for three level diode clamped voltage source inverter, *Int. J. Power Electronics and Drive System*, 5(1), 15-23. https://doi.org/10.11591/ijpeds.v5i1.6038.

[3] V. Rajasekar and S. Selvarajan. 2015. Log Gabor filter for image based vehicle verification, *Int. J. Applied Engg. Research*, 10(16), 7783-7789.

[4] S. Ramachandran, S. Jaganathan and M. Elakkiya. 2015. ETA algorithm for vehicle positioning and GSM based securing message through vehicle to infrastructure communication, *Int. J. Applied Engg. Research*, 10(16), 8627-8631.

[5] C. Sarath and A. Antony. 2015. Implementation of SVM to improve the performance of a nine level inverter with reduced number of switches, *Proc. IEEE Int. Conf. Signal Processing, Informatics, Communication & Energy Systems*, 1-5. https://doi.org/10.1109/SPICES.2015.7091445.